U.S. DEPARTMENT OF ENERGY

Sandia National Laboratories

Scott T. Broome
Senior Member of the Technical Staff
Geomechanics Department 6914

Albuquerque, NM 87185-1033
Phone: (505) 845-0541
Fax: (505) 284-5756
e-mail:stbroom@sandia.gov

date: April 16, 2013

to: Aviva Sussman (LANL), Christopher Bradley (LANL), Wendee Brunish (LANL), Tarabay Antoun (LLNL), Margaret Townsend (NSTec), Catherine Snelson (NSTec)

from: Scott Broome, Moo Lee (SNL, 6914)

Subject: **Dynamic Brazilian tension results on core from borehole U-15n, Nevada National Security Site, in support of NCNS Source Physics Experiment**

Summary

Dynamic Brazilian tension (DBR) tests from core hole U-15n are part of a larger material characterization effort for the Source Physics Experiment (SPE) project. This larger effort encompasses characterizing Climax Stock granite rock from the Nevada National Security Site (NNSS) both before and after each SPE shot.

Core hole U-15n is the vertically oriented source hole for all SPE shots; pre shot core was taken from this hole for DBR testing. The first shot (SPE-1) conducted on May 3, 2011 was a calibration shot. SPE-1 was an order of magnitude smaller than the second shot (SPE-2). After SPE-2 was conducted on October 25, 2011 an inclined core hole (U-15n#10) was drilled. At its bottom, the inclined corehole intersects the source hole. Geomechanical tests from U-15n#10 are either in progress or have been completed. The third shot (SPE-3) occurred on July 24, 2012. Vertical and angled core holes were drilled post SPE-3 and samples will soon be selected for Geomechanical characterization. At the time of this writing, work is ongoing at the NNSS in preparation for the fourth SPE shot (SPE-4).

Tests completed to date or are in progress on material from U-15n (pre SPE shots 1, 2, and 3) include the following:

1) Unconfined Compression (Broome and Pfeifle, 2011)
2) Direct Shear (tests completed; report in progress)
3) Dynamic Brazilian Tension (current report)
4) Triaxial Shear on natural fractures (in progress)
5) Triaxial Compression (Broome and Lee, 2013)

Tests completed to date or are in progress on material from U-15n#10 (post SPE-2 and pre SPE-3) include the following:

1) Unconfined Compression (Broome and Lee, 2012)
2) Direct Shear (tests completed; report in progress)
3) Triaxial Compression (in progress)

The current test series includes DBR tests on fault material and intact granite; Table 1 shows a summary of results including sample #, depth, density, tensile strength, material type, and average dynamic Young's modulus and Poisson's ratio.

Table 1: Sample #, depth, density, tensile strength, material type, average dynamic Young's modulus, and average dynamic Poisson's ratio.

Sample #	Depth (ft)	Depth (m)	Density (g/cc)	Tensile Strength (MPa)	Material	$E_{dynamic}$ (GPa)	$\nu_{dynamic}$
SPE-BR-01	87.2	26.6	2.55	13.67	Fault Mat.	46.62	0.20
SPE-BR-02	84.9	25.9	2.58	16.59	Fault Mat.	51.51	0.19
SPE-BR-03	84.7	25.8	2.57	14.12	Fault Mat.	47.23	0.17
SPE-BR-04	76.5	23.3	2.53	13.44	Fault Mat.	43.93	0.22
SPE-BR-05	149.9	45.7	2.64	30.20	Intact	72.48	0.24
SPE-BR-06	151	46.0	2.63	32.28	Intact	77.37	0.24
SPE-BR-07	151.8	46.3	2.66	34.24	Intact	82.72	0.23

Background

The NNSS serves as the geologic setting for the SPE program. The SPE tests provideground truth data to create and improve strong ground motion and seismic S-wave generation and propagation models. The NNSS was chosen as the test bed because it provides a variety of geologic settings ranging from relatively simple to very complex.

Each series of SPE testing will comprise the setting and firing of chemical explosive charges (source) placed in a central borehole at varying depths and recording ground motions in instrumented boreholes located in two rings around the source, positioned at different radii. Modeling using advanced simulation codes will be performed both before and after each test to predict ground response and to improve models based on acquired field data, respectively.

A key component in the predictive capability and ultimate validation of the models is the full understanding of the intervening geology between the source and the instrumented boreholes including the geomechanical behavior of the site's rock/structural features. This memorandum reports on dynamic Brazilian tension testing of cores retrieved from U-15n.

All DBR testing reported upon herein originated from U-15n core hole before any SPE shot was conducted; the core hole is drilled in granitic rock (quartz monzonite). U-15n core hole was

drilled at the location of the central SPE borehole, and thus closely represents material in which the explosive charges have occurred. As shown in Figure 1 from Townsend, et al. (2012), there are two fault zones within U-15n. Fault #1 and Fault #2 intersect U-15n at depths of approximately 82 feet and 107 feet respectively. Specimens for DBR tests were selected from two distinct depth regions; one of these regions corresponds to Fault #1 and the other region is around a depth of 150 feet and is strong intact granite. Thus far, the U-15n location has been the site of three SPE's (SPE-1, SPE-2, and SPE-3) in Area 15 of the NNSS. The fourth SPE shot is scheduled in the late 2013 timeframe.

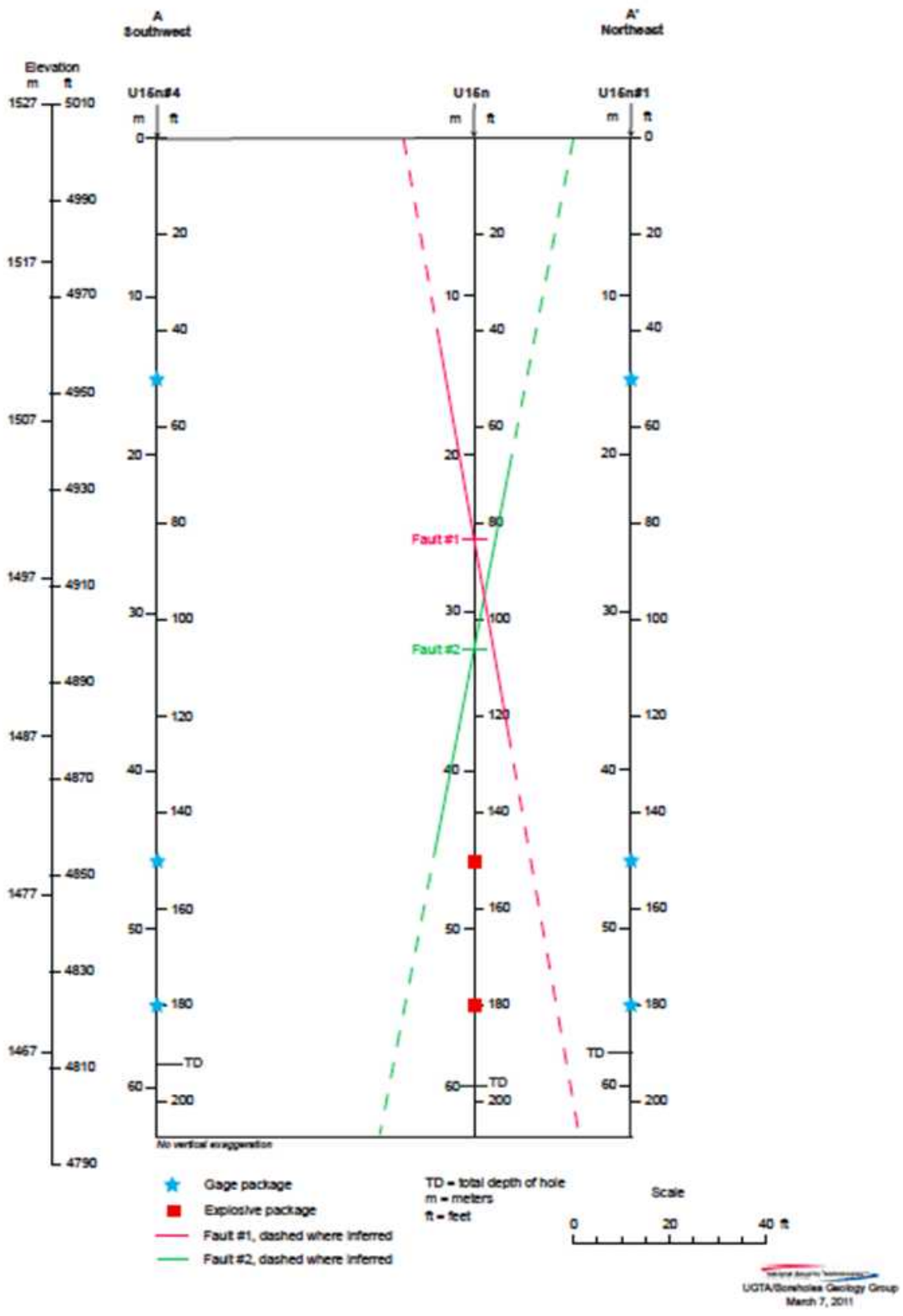

Figure 1: Diagram of source Core hole U-15n with faults intersecting at depths of 82 and 107 feet.

Specimen Preparation and Experimental Methods

Specimen Preparation

Test specimens (right circular cylinders) were prepared from the 63.5 mm (2.5 inch) diameter field core by cutting them to approximate length using a standard rock saw, turning the core down to ~50.8 mm (2.0 inches) on a lathe, and then grinding the ends flat and parallel to final length such that the length-to-diameter ratio, L:D, on each test specimen is 1:2 (Figure 2). Two types of rock were tested; intact and fault material. Intact specimens were turned down on the lathe dry and both the sawing and the grinding operations used standard tap water for cooling. All preparation steps for fault material specimens were performed dry.

Specimens were sized to provide representative results given the maximum grain size of this granite ranges from 0.5-6.35 mm (0.02-0.25 in). Phenocrysts in small quantities were observed along the core length and are as large as ~25.4 mm (1.0 inch) across. The specimen diameter of two inches is slightly less than ten times the maximum observed grain size, however this diameter was necessary for compatibility with the ~25.4 mm (1.0 inch) diameter incident and transmission bars on the Split Hopkinson Pressure Bar (SHPB) device used for these high strain rate tests. Figure 3 shows a specimen mounted between the incident and transmission bars on the SHPB bar device and the general testing setup of the SHPB bar experiment along with a schematic representation of the wave trains obtained from the strain response of the incident and transmission bars.

The dimensions and mass of each specimen were measured to determine specimen density. Field cores used in preparing the test specimens were selected from primarily two depths; fault material specimens were near the fault zone at 82 feet depth (Figure 1) and intact specimens were from ~150 feet depth. These two distinct depth regions were chosen to represent the end members of the range of strength observed from previous triaxial (confined and unconfined) compression testing.

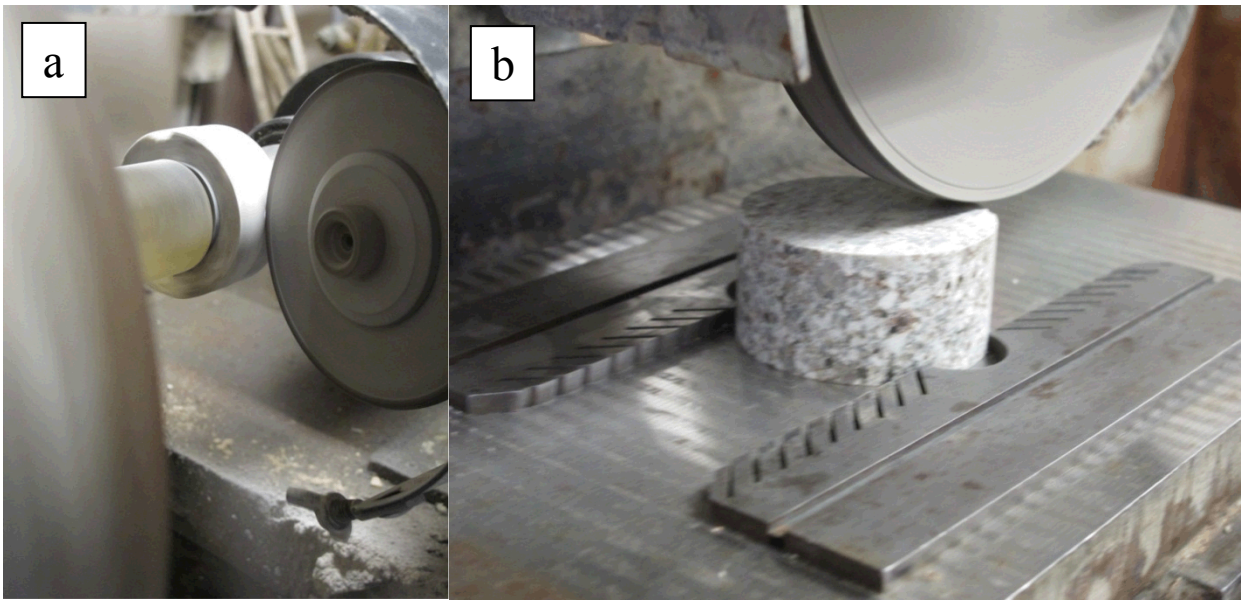

Figure 2: Sample preparation steps: a) turning core down to 50.8 mm on a lathe and b) grinding ends to tolerance.

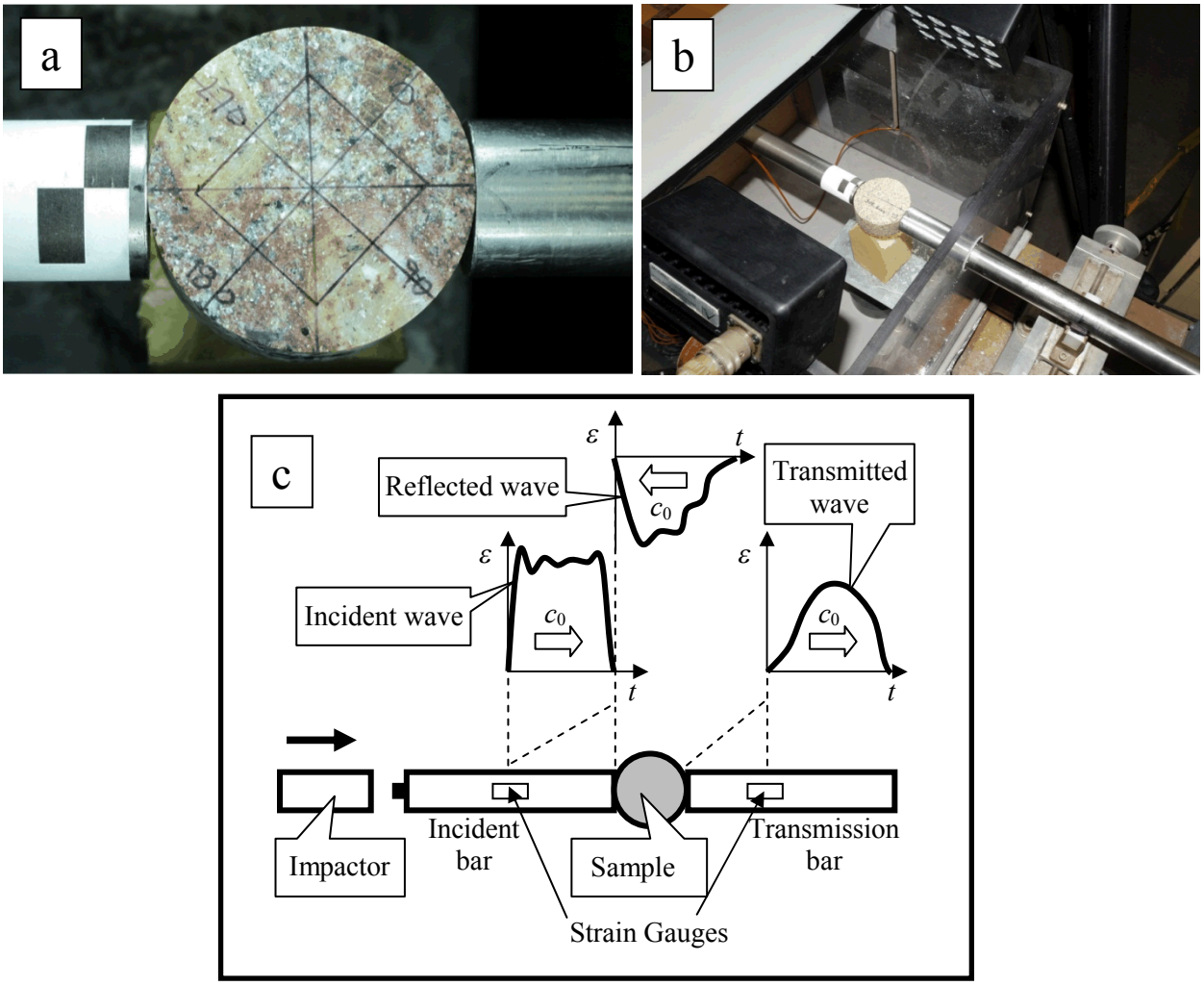

Figure 3: Specimen ready for testing mounted between the incident and transmission bars (a and b) and setup of the SHPB experiment and schematic representation of the wave trains (c).

Bulk Density Determination

The bulk density of each DBR test specimen was determined from its mass and volume; volume is calculated using dimensional measurements assuming a right-circular-cylindrical geometry. Specimens were tested with as received moisture content; pre-test core was stored inside at ~22˚C with relative humidity ranging from 5% to 40%.

Dynamic Brazilian Disc Tension Testing

During the SNL/LANL SHPB experiment, a prepared test sample was placed between two bars, as shown in Figure 3. The bar on the left is called the incident bar, while the bar on the right is called the transmission bar. The pressure pulse is generated on the left hand side of the incident bar by the action of a striker bar (Figure 3c). The general test setup is shown in Figure 4 and

shows the high speed photography equipment along with the SHPB data acquisition equipment. Due to strain rates on the order of 1E+02 sec^{-1}, sample failure can be quite explosive as shown in Figure 5.

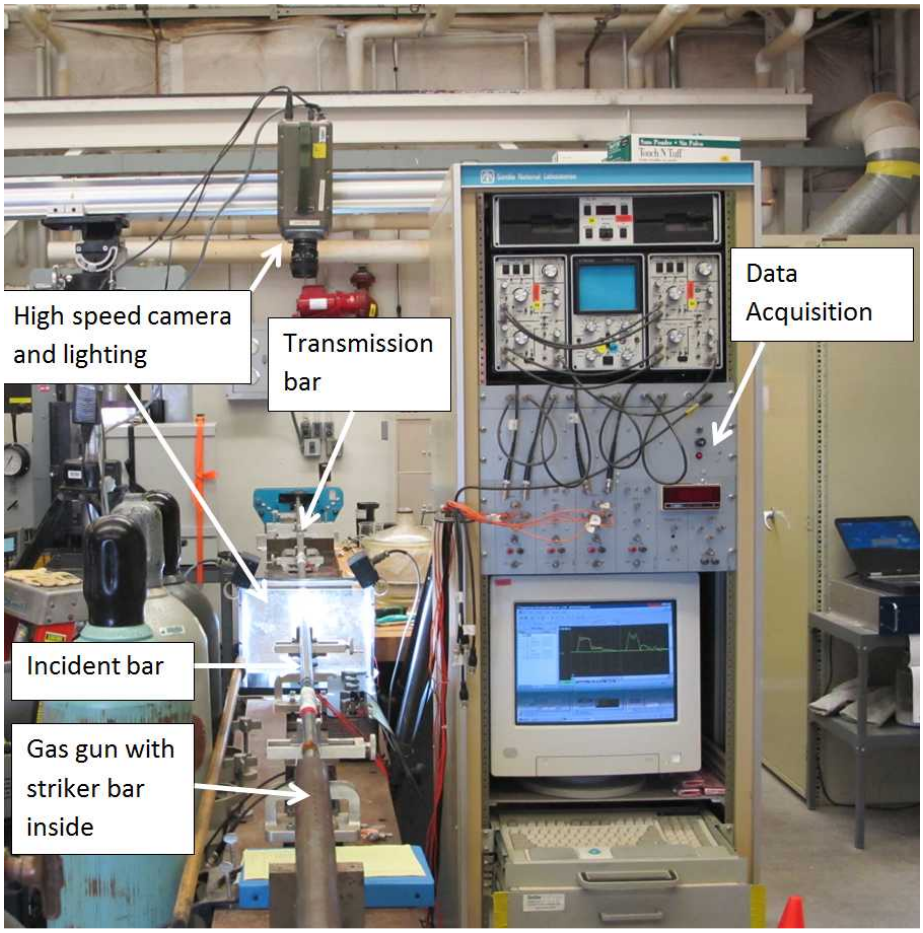

Figure 4: General test setup with the Split Hopkinson Pressure Bar.

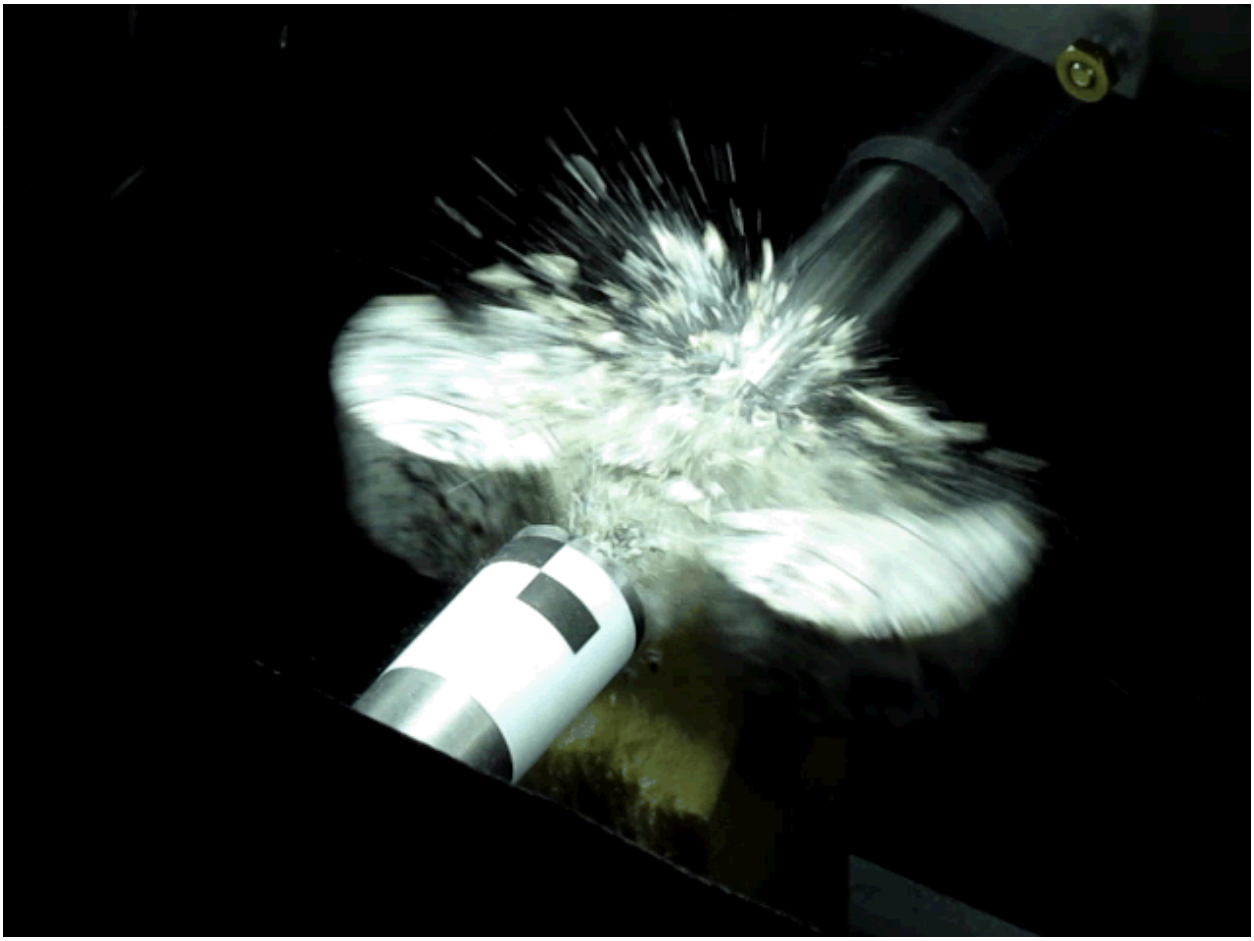

Figure 5: Explosive failure of sample SPE-BR-02.

In order to obtain a desired pressure pulse shape a small piece of felt metal is placed on the free end of the incident bar (Figure 6). The striker travels at a certain velocity and hits the felt metal, which deforms and transmits the modified pressure wave to the incident bar. The length and the amplitude of the resulting pressure pulse are governed by the length, weight, and speed of the striker respectively (Chen and Song, 2011). Two strain gauges are placed along the length of the incident and transmission bar. The strain gauge locations on the incident and transmission bars are 1028 mm (40.5 inches) and 203 mm (8.0 inches) from the sample respectively. The strain gauge on the incident bar measures the strain wave travelling from the free end to the sample that is a result of the impact (incident wave) and the strain wave travelling from the sample to the free end that is a result of the incident wave reflection from the bar-sample interface (reflected wave). The strain gauge on the transmission bar measures the transmitted strain wave travelling from the sample to the free end (transmitted wave).

The incident and the transmission bars are supported to avoid any lateral movement and to allow only longitudinal movement. Because of this, the stress state in these bars can be described by the one dimensional wave equation (Chen and Song, 2011). The displacement as a function of time for a given point along the bars is given by

$$u = c_0 \int_0^t \varepsilon \, dt \tag{1}$$

where ε is the strain in the bar and c_0 is the elastic wave speed in the bar given by

$$c_0 = \sqrt{\frac{E}{\rho}} \tag{2}$$

while E is the Young's modulus and ρ is the density of the bar.

Due to the fact that the incident and reflected waves travel in opposite directions, the displacement at the interface between the incident bar and the sample is obtained as a combination of the effects of these two waves, as follows (Chen and Song, 2011)

$$\begin{aligned} u_1 &= c_0 \int_0^t \varepsilon_i \, dt - c_0 \int_0^t \varepsilon_r \, dt \\ &= c_0 \int_0^t \left(\varepsilon_i - \varepsilon_r \right) dt \end{aligned} \tag{3}$$

where ε_i and ε_r are the strains due to the incident and reflected waves respectively. On the other hand, the displacement at the interface between the sample and the transmission bar is solely dictated by the transmitted wave, as follows

$$u_2 = c_0 \int_0^t \varepsilon_t \, dt \tag{4}$$

where ε_t is the strain due to the transmitted wave. Following this line of reasoning, the contact surface between the incident bar and the sample moves at velocity v_1, which is given by

$$v_1 = \frac{\partial u_1}{\partial t} = c_0 \left(\varepsilon_i - \varepsilon_r \right) \tag{5}$$

while the contact surface between the sample and the transmission bar moves at velocity v_2, which is given by

$$v_2 = \frac{\partial u_2}{\partial t} = c_0 \varepsilon_t \tag{6}$$

Incident and transmission bar velocities for a typical sample are plotted versus time in Figure 7.

As shown in Figure 8, for the SHPB Brazilian experiment presented here, we will assume that the sample is under quasi-static conditions (see Dai and Xia, 2009 for a detailed description of the quasi-static enforcement) and the tensile stress of the sample material is related to the average compressive force infringed by the incident and the transmission bars as follows

$$\sigma_t = \frac{2 f(t)}{\pi d b} \tag{7}$$

where $f(t)$ is the time evolution of the average compressive force and d and b are the diameter and thickness of the sample, respectively. Tension is denoted as a positive quantity throughout this report.

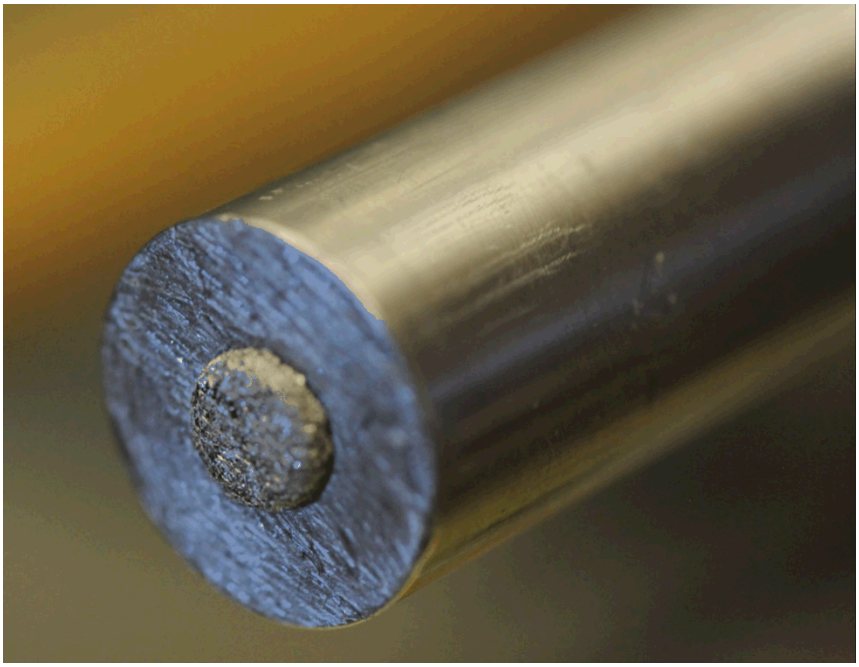

Figure 6: Felt metal used as a pulse shaper placed on the end of the incident bar.

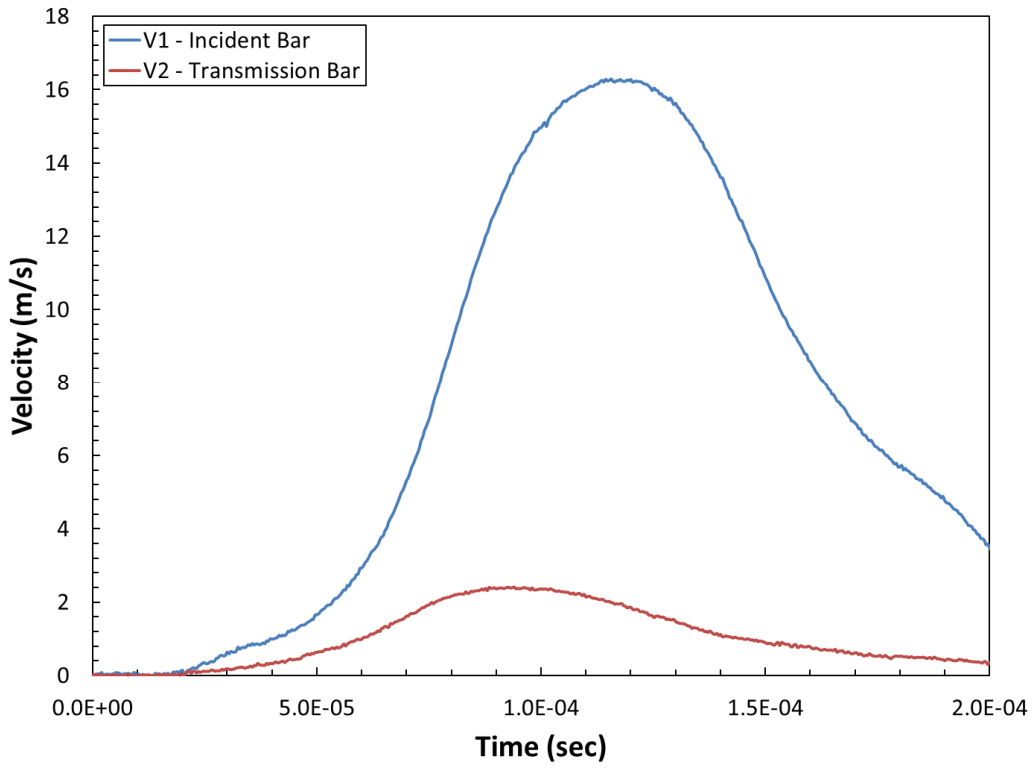

Figure 7: Typical velocity versus time plot.

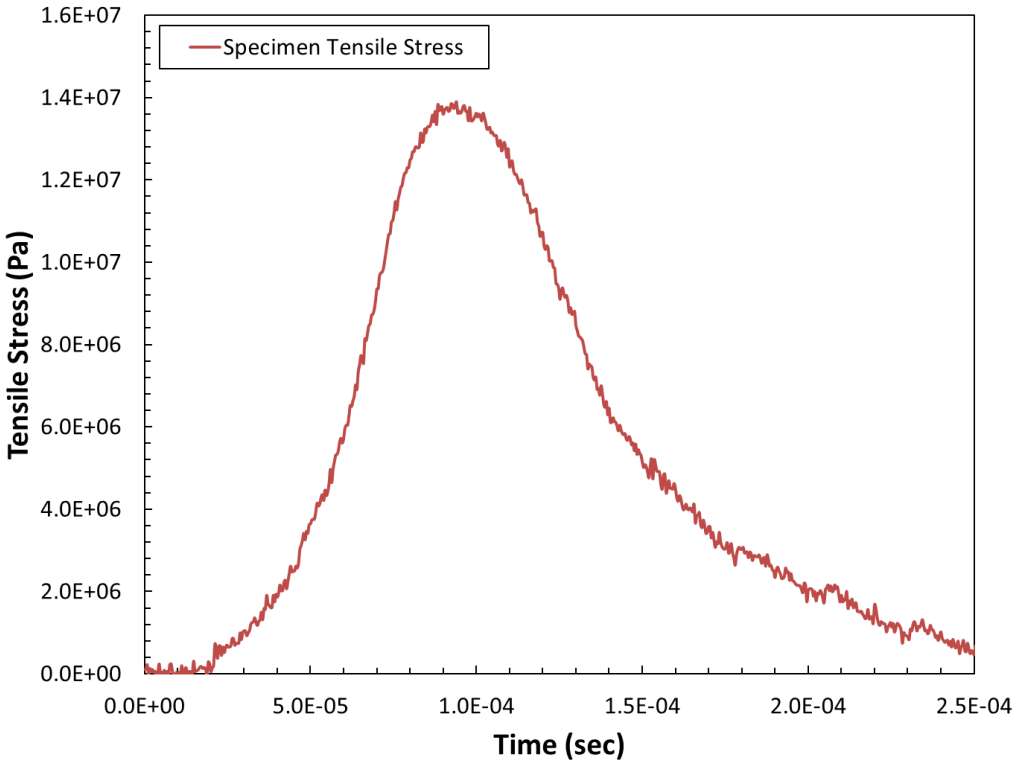

Figure 8: Typical tensile stress versus time plot.

Note that much of the text on pages nine and ten showing the development of velocity and stress equations and Figure 3c were taken from Rougier et al., 2011.

Compressional and Shear Wave Velocity Measurements

Ultrasonic compressional and shear wave velocity measurements, V_p and V_s, were performed on each DBR specimen under ambient conditions prior to testing. As shown in Figure 9, wave speed measurements were made coincident with each specimen axis and also orthogonal to the axis across four diameters separated by 45^0. Test orientation was determined based on results from wave speed measurements made coincident with the specimen axis; specimens were tested 90˚ to the slowest velocity measurement to give the most conservative (weakest) measurement as illustrated in Figure 10.

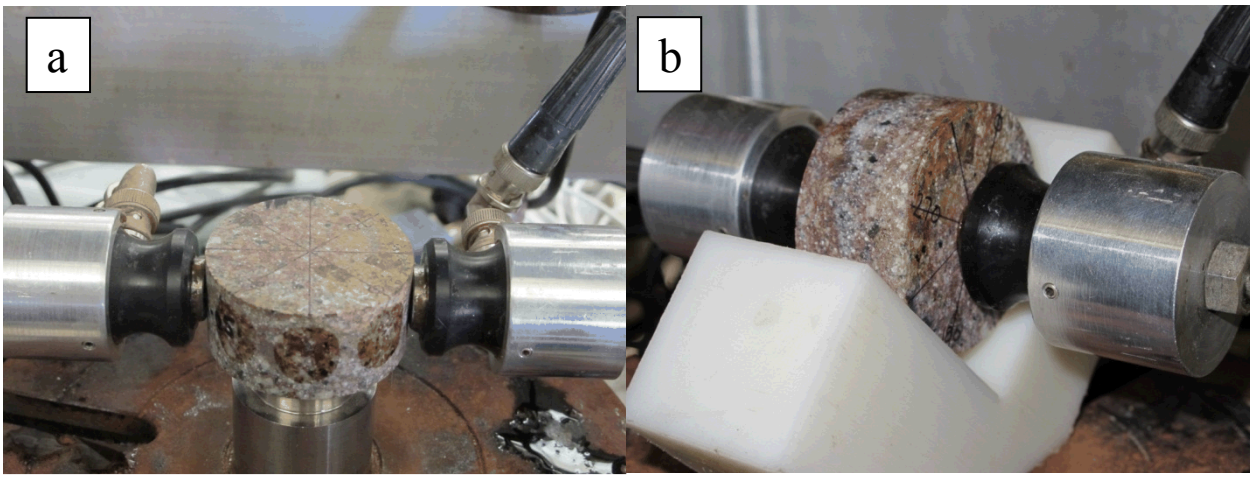

Figure 9: Ultrasonic compressional and shear wave velocity measurements performed both: a) orthogonal to the specimen axis and b) coincident to the specimen axis.

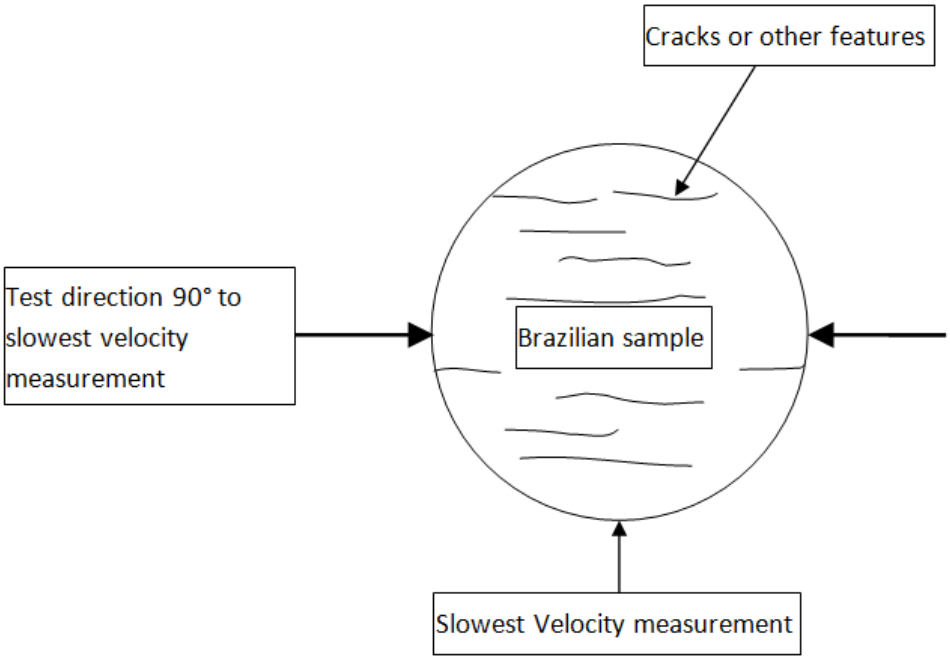

Figure 10: Methodology for determination of DBR sample test direction.

Experimental Results

Table 1 gives P and S wave velocity measurements taken across four diameters and through one thickness of each specimen and gives the test direction based on the lowest P velocity; sample depth, weight, density and dimensions are also included.

Six plots are shown in the Appendix for each specimen. These plots are generated from the strain data received from the incident and transmission bars; the plots are:

1. Voltage versus time
2. Strain versus time
3. Velocity versus time
4. Strain rate versus time
5. Stress versus time
6. Specimen tensile stress versus time

Figure 11 shows two plots with data plotted on the same scale. The first plot is voltage versus time data from a fault material specimen and the second plot is voltage versus time data from an intact specimen. The intact specimen exhibits higher voltage in the transmission wave than the fault material specimen. Because the intact material is harder and stronger, more strain energy is "transmitted" from the incident bar to the transmission bar. Note the flattening of the slope of the curve at ~ -0.01 Volts for the reflected wave for the intact specimen. The flattening of the slope in the reflected wave indicates a region of constant strain rate in the sample (Chen and Song, 2011). Constant strain rate loading is not observed for the fault material specimens. The plots in Figure 11 are the beginning point of data reduction; strain gauge voltage data is multiplied by strain gauge sensitivities (0.0515 and 0.0520 for incident and transmission bar strain gauges) to convert to the engineering unit of strain.

Figure 12 shows specimen tensile stress versus time for all dynamic Brazilian disc tension tests. Tensile stress averages ~32 MPa (4640 psi) for intact specimens and ~14 MPa (2030 psi) for fault material specimens. The average loading rate is given for the two material types investigated. The gas gun pressure used to propel the striker bar was held constant at 0.2 MPa (30 psi) and therefore the difference in loading rates given in Figure 12 (920 GPa/sec (133.4 msi) and 353 GPa/sec (51.2 msi) for intact and fault materials) are directly related to the strength and stiffness of the specimens.

The time for the specimens to reach peak tensile stress averaged 40 μs. High speed photography shown in ~20 μs increments (Figure 13) shows the evolution of cracks developing within the specimen on fault material. The first photo in the sequence shows the sample a few microseconds before initial loading and after the third photo in the series, peak stress has been achieved.

Table 1: Sample #, Depth, Weight, Density and Velocity measurements taken showing test direction relating to P-wave velocity.

Sample											
Depth (ft)											
Weight (g)				Corrected	Corrected						Avgerage Dia. (mm)
Density (g/cc)	Pt / angle	P wave (μs)	S wave (μs)	P wave (μs)	S wave (μs)	Length (in)	P velocity in / μs	P velocity mm / μs	S velocity in / μs	S velocity mm / μs	Thickness (mm)
SPE-BR-01	1 / 0°	11.70	19.07	11.43	18.80	1.999	0.1749	4.442	0.1063	2.701	
87.2	2 / 45°	11.78	18.49	11.51	18.22	2.000	0.1738	4.414	0.1098	2.788	
129.56	3 / 90°	11.53	18.32	11.26	18.05	2.000	0.1776	4.512	0.1108	2.814	
2.55	4 / 135°	11.27	18.40	11.00	18.13	2.000	0.1818	4.618	0.1103	2.802	50.79
	5 / axial	5.71	9.56	5.44	9.29	0.989	0.1818	4.618	0.1065	2.704	25.12
SPE-BR-02	1 / 0°	11.60	18.66	11.33	18.39	1.997	0.1763	4.477	0.1086	2.758	
84.9	2 / 45°	11.94	18.63	11.67	18.36	1.997	0.1711	4.347	0.1088	2.763	
132.66	3 / 90°	10.92	17.25	10.65	16.98	1.997	0.1875	4.763	0.1176	2.987	
2.58	4 / 135°	11.10	17.36	10.83	17.09	1.997	0.1844	4.684	0.1169	2.968	50.72
	5 / axial	5.07	8.83	4.80	8.56	1.002	0.2087	5.301	0.1171	2.973	25.45
SPE-BR-03	1 / 0°	11.87	18.26	11.60	17.99	1.997	0.1722	4.373	0.1110	2.820	
84.7	2 / 45°	11.80	18.47	11.53	18.20	1.998	0.1733	4.401	0.1098	2.788	
132.44	3 / 90°	11.68	18.40	11.41	18.13	1.998	0.1751	4.448	0.1102	2.799	
2.57	4 / 135°	11.99	18.15	11.72	17.88	1.998	0.1705	4.330	0.1117	2.838	50.74
	5 / axial	5.55	9.52	5.28	9.25	1.003	0.1900	4.825	0.1084	2.754	25.48
SPE-BR-04	1 / 0°	12.42	19.51	12.15	19.24	1.996	0.1643	4.173	0.1037	2.635	
76.5	2 / 45°	12.17	19.08	11.90	18.81	1.996	0.1677	4.260	0.1061	2.695	
128.05	3 / 90°	10.75	18.66	10.48	18.39	1.996	0.1905	4.838	0.1085	2.757	
2.53	4 / 135°	11.99	19.05	11.72	18.78	1.996	0.1703	4.326	0.1063	2.700	50.70
	5 / axial	5.41	10.04	5.14	9.77	0.986	0.1918	4.872	0.1009	2.563	25.04
SPE-BR-05	1 / 0°	8.88	15.17	8.61	14.90	1.998	0.2321	5.894	0.1341	3.406	
149.9	2 / 45°	9.09	14.99	8.82	14.72	1.998	0.2265	5.754	0.1357	3.448	
135.72	3 / 90°	9.21	15.18	8.94	14.91	1.998	0.2235	5.677	0.1340	3.404	
2.64	4 / 135°	9.19	15.54	8.92	15.27	1.998	0.2240	5.689	0.1308	3.323	50.75
	5 / axial	4.86	8.69	4.59	8.42	0.999	0.2176	5.528	0.1186	3.014	25.37
SPE-BR-06	1 / 0°	8.87	15.10	8.60	14.83	2.000	0.2326	5.907	0.1349	3.425	
151.0	2 / 45°	8.90	15.00	8.63	14.73	2.000	0.2317	5.886	0.1358	3.449	
135.25	3 / 90°	8.82	14.91	8.55	14.64	2.001	0.2340	5.944	0.1367	3.472	
2.63	4 / 135°	8.98	15.08	8.71	14.81	2.001	0.2297	5.835	0.1351	3.432	50.81
	5 / axial	4.58	7.65	4.31	7.38	0.998	0.2316	5.881	0.1352	3.435	25.35
SPE-BR-07	1 / 0°	8.56	14.66	8.29	14.39	2.000	0.2413	6.128	0.1390	3.530	
151.8	2 / 45°	8.66	14.64	8.39	14.37	2.000	0.2384	6.055	0.1392	3.535	
136.63	3 / 90°	8.87	14.48	8.60	14.21	2.000	0.2326	5.907	0.1407	3.575	
2.66	4 / 135°	8.75	14.46	8.48	14.19	2.000	0.2358	5.991	0.1409	3.580	50.80
	5 / axial	4.44	7.44	4.17	7.17	0.999	0.2396	6.085	0.1393	3.539	25.37

Selection; lowest velocity
Direction of test

Note re corrections: (average) trigger delay/offset (0.03 μs) and total platen correction (0.24 μs) subtracted from times.

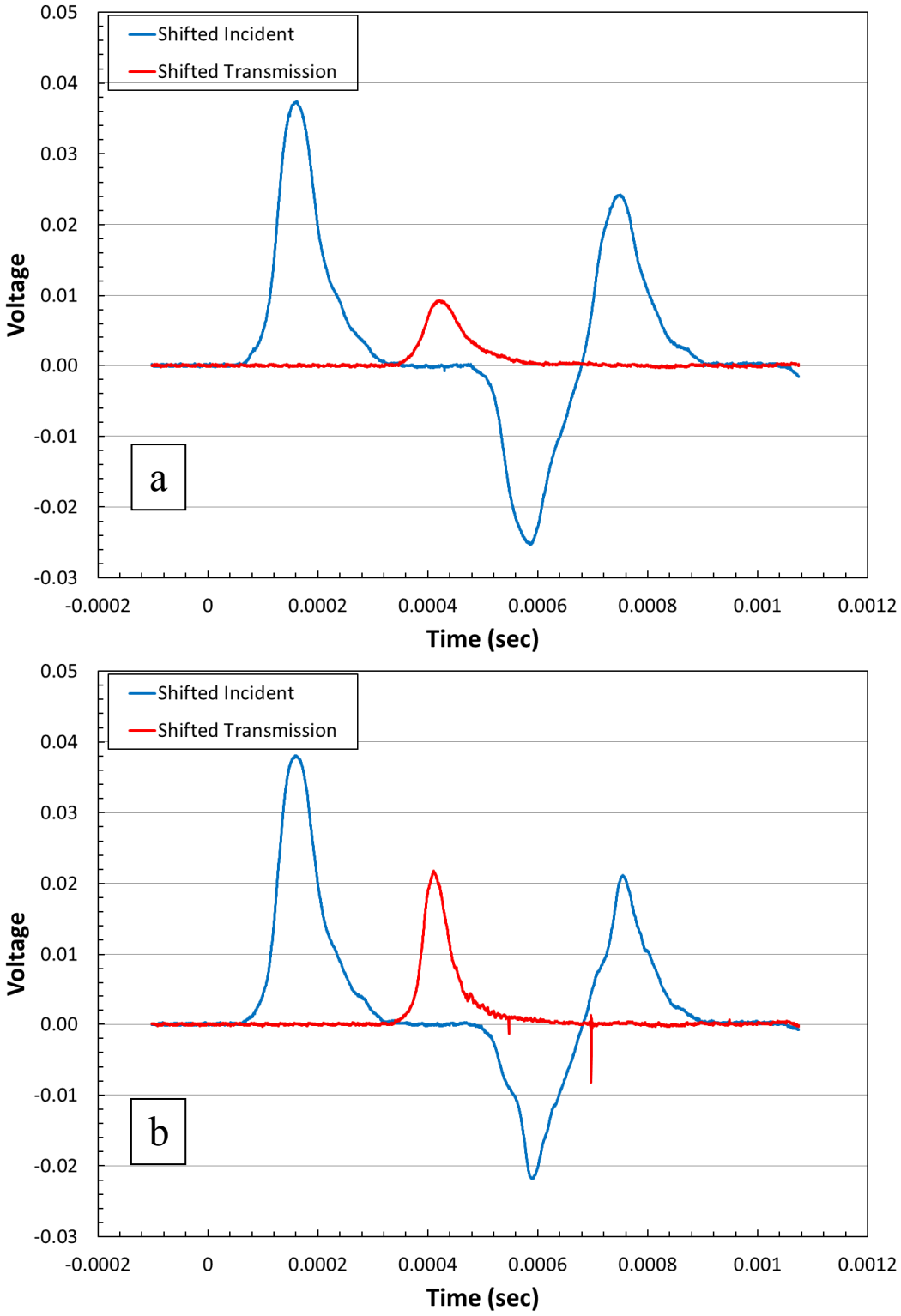

Figure 11: Voltage versus time for a) fault material specimen and b) intact specimen.

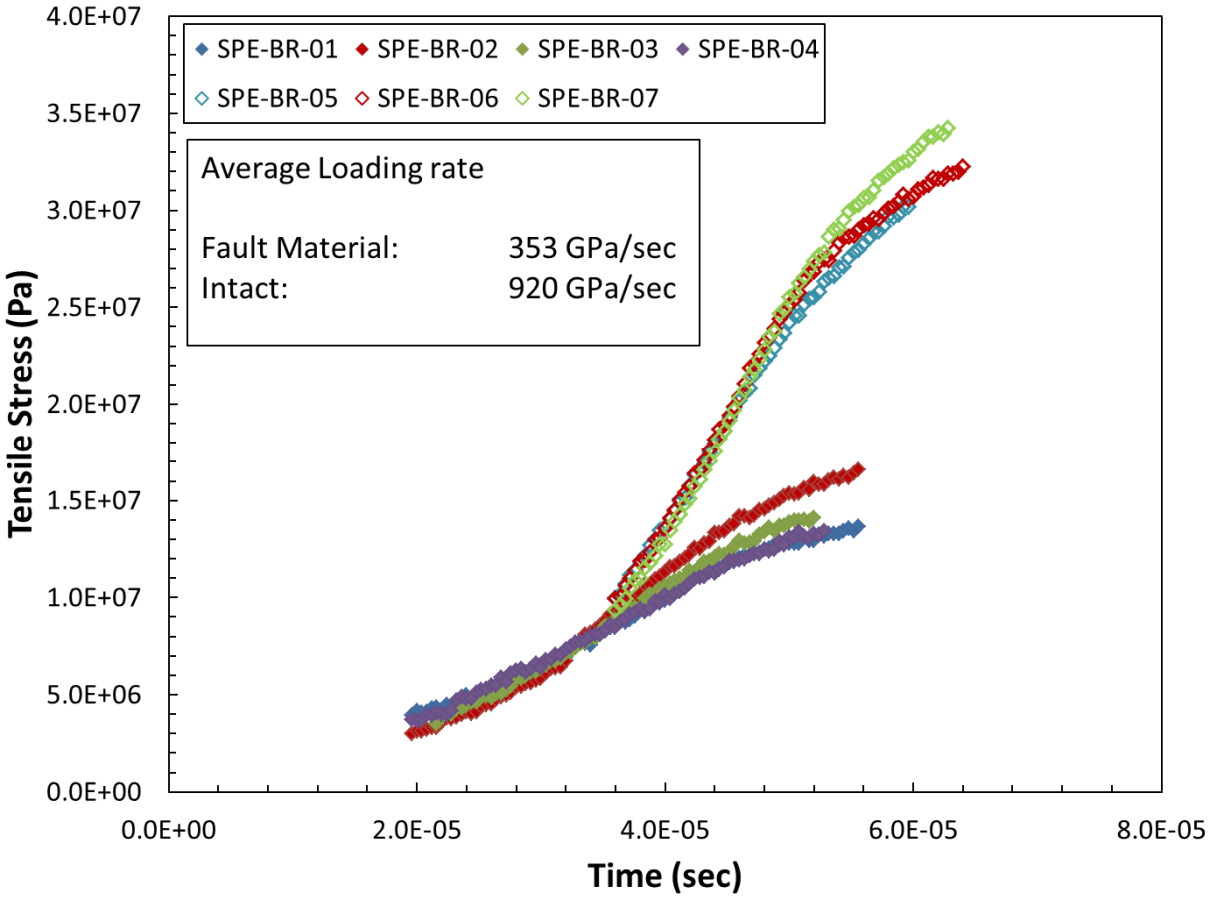

Figure 12. Tensile Stress versus time for all dynamic Brazilian tests.

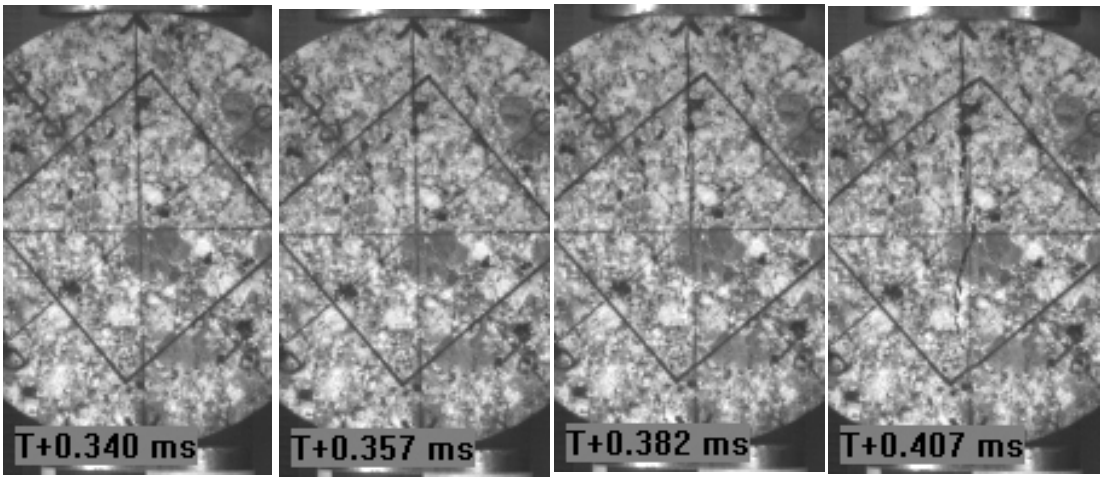

Figure 13: Images from high speed photography showing fracture evolution in ~20μs increments on a fault material specimen.

Dynamic elastic Young's modulus, $E_{dynamic}$, was determined directly from:

$$E_{dynamic} = \frac{\rho V_S^2 \left(3V_P^2 - 4V_S^2\right)}{\left(V_P^2 - V_S^2\right)}$$

where ρ is the sample density and V_P and V_S are the compressional and shear wave velocities, respectively. Values of dynamic elastic Poisson's ratio, $\nu_{dynamic}$, were calculated from:

$$\nu_{dynamic} = \frac{\left(V_P^2 - 2V_S^2\right)}{2\left(V_P^2 - V_S^2\right)}$$

Table 2 shows values of $E_{dynamic}$ and ν for each velocity measurement taken on each sample. The green Pt/angle cells indicate test direction. The average dynamic Young's modulus and dynamic Poisson's ratio for the fault material are 47.3 GPa and 0.20. The average dynamic Young's modulus and dynamic Poisson's ratio for the intact material are 77.5 GPa and 0.24. These values compare well with measurements taken on similar material types for triaxial compression tests reported in Broome and Lee, 2013.

Table 2: Dynamic Young's modulus and Poisson's ratio for each velocity measurement on each dynamic Brazilian tension test.

Fault material				**Intact**			
Sample	Pt / angle	$E_{dynamic}$	ν	Sample	Pt / angle	$E_{dynamic}$	ν
		GPa				GPa	
SPE-BR-01	1 / 0º	44.81	0.21	SPE-BR-05	1 / 0º	76.65	0.25
	2 / 45°	46.22	0.17		2 / 45°	76.68	0.22
	3 / 90°	47.64	0.18		3 / 90°	74.71	0.22
	4 / 135°	48.31	0.21		4 / 135°	72.49	0.24
	5 / axial	46.12	0.24		5 / axial	61.89	0.29
SPE-BR-02	1 / 0º	46.87	0.19	SPE-BR-06	1 / 0º	76.98	0.25
	2 / 45°	45.72	0.16		2 / 45°	77.53	0.24
	3 / 90°	54.13	0.18		3 / 90°	78.72	0.24
	4 / 135°	52.92	0.16		4 / 135°	76.58	0.24
	5 / axial	57.94	0.27		5 / axial	77.06	0.24
SPE-BR-03	1 / 0º	46.77	0.14	SPE-BR-07	1 / 0º	82.88	0.25
	2 / 45°	46.56	0.16		2 / 45°	82.43	0.24
	3 / 90°	47.22	0.17		3 / 90°	82.23	0.21
	4 / 135°	46.53	0.12		4 / 135°	83.23	0.22
	5 / axial	49.08	0.26		5 / axial	82.81	0.24
SPE-BR-04	1 / 0º	41.09	0.17				
	2 / 45°	42.92	0.17				
	3 / 90°	48.49	0.26				
	4 / 135°	43.60	0.18				
	5 / axial	43.56	0.31				
	Average	47.32	0.20		Average	77.52	0.24

Conclusions

Seven dynamic Brazilian disc tension tests from core hole U-15n (the source hole for all SPE shots) have been presented and discussed. All tests were from pre shot core with two material types tested; fault material and intact granite. The tensile strength for the fault material and intact granite averaged 14.5 and 32.2 MPa respectively. Dynamic Young's modulus and Poisson's ratio averaged 47.3 MPa and 0.20 for fault material and 77.52 MPa and 0.24 for intact granite. The average density for fault material specimens was 2.56 g/cc while intact granite specimen average density was 2.64 g/cc.

Dynamic Brazilian Tension tests from core hole U-15n are part of a larger material characterization effort for the Source Physics Experiment (SPE) project. This larger effort encompasses characterizing Climax Stock granite rock from the Nevada National Security Site (NNSS) both before and after each SPE shot.

Tests completed to date or are in progress on material from U-15n (pre any SPE shots) include the following:

1) Unconfined Compression (Broome and Pfeifle, 2011)
2) Direct Shear (tests completed; report in progress)
3) Dynamic Brazilian Tension (current report)
4) Triaxial Shear on natural fractures (in progress)
5) Triaxial Compression (Broome and Lee, 2013)

Tests completed to date or are in progress on material from U-15n#10 (post SPE-2 and pre SPE-3) include the following:

1) Unconfined Compression (Broome and Lee, 2012)
2) Direct Shear (tests completed; report in progress)
3) Triaxial Compression (in progress)

References

Broome, S. and Pfeifle, T., 2011. Phase 1 Mechanical Property Test Results for Borehole U-15n in Support of NCNS Source Physics Experiment, SAND2011-4394C.

Broome, S. and Lee, M., 2012. Unconfined Compression Mechanical Testing Results on Core from Borehole U-15n#10, Nevada National Security Site, in support of NCNS Source Physics Experiment, SAND2012-9376P.

Broome, S. and Lee, M., 2013. Triaxial compression testing results on core from borehole U-15n, Nevada National Security Site, in support of NCNS Source Physics Experiment, SAND2013-2913P.

Townsend, M., et al., 2012. Projected Extent of Two Faults Encountered in Core Hole U-15n, NSTec UGTA/Boreholes Geology Group, 08 March 2011.

Chen, W.W. and Song, B. 2011. Split Hopkinson (Kolsky) Bar Design, Testing and Applications, Springer Science+Business Media, LLC.

Dai, F. and K. Xia. 2009. Tensile strength anisotropy of Barre Granite. In RockEng09: 3rd Canada-US rock mechanics symposium, Toronto - Canada, 9 – 15 May 2009, eds. C.S. Diederichs and Grasselli, 231-232.

Rougier, E., et al., 2011. The Combined Finite-Discrete Element Method applied to the Study of Rock Fracturing Behavior in 3D. ARMA 11-517: In 45th U.S. Rock Mechanics/Geomechanics Preceding, Chicago, 2011.

Plots of Voltage, Strain, Velocity, Strain rate, Stress, and Sample tensile stress versus time for all dynamic Brazilian disc tension tests.

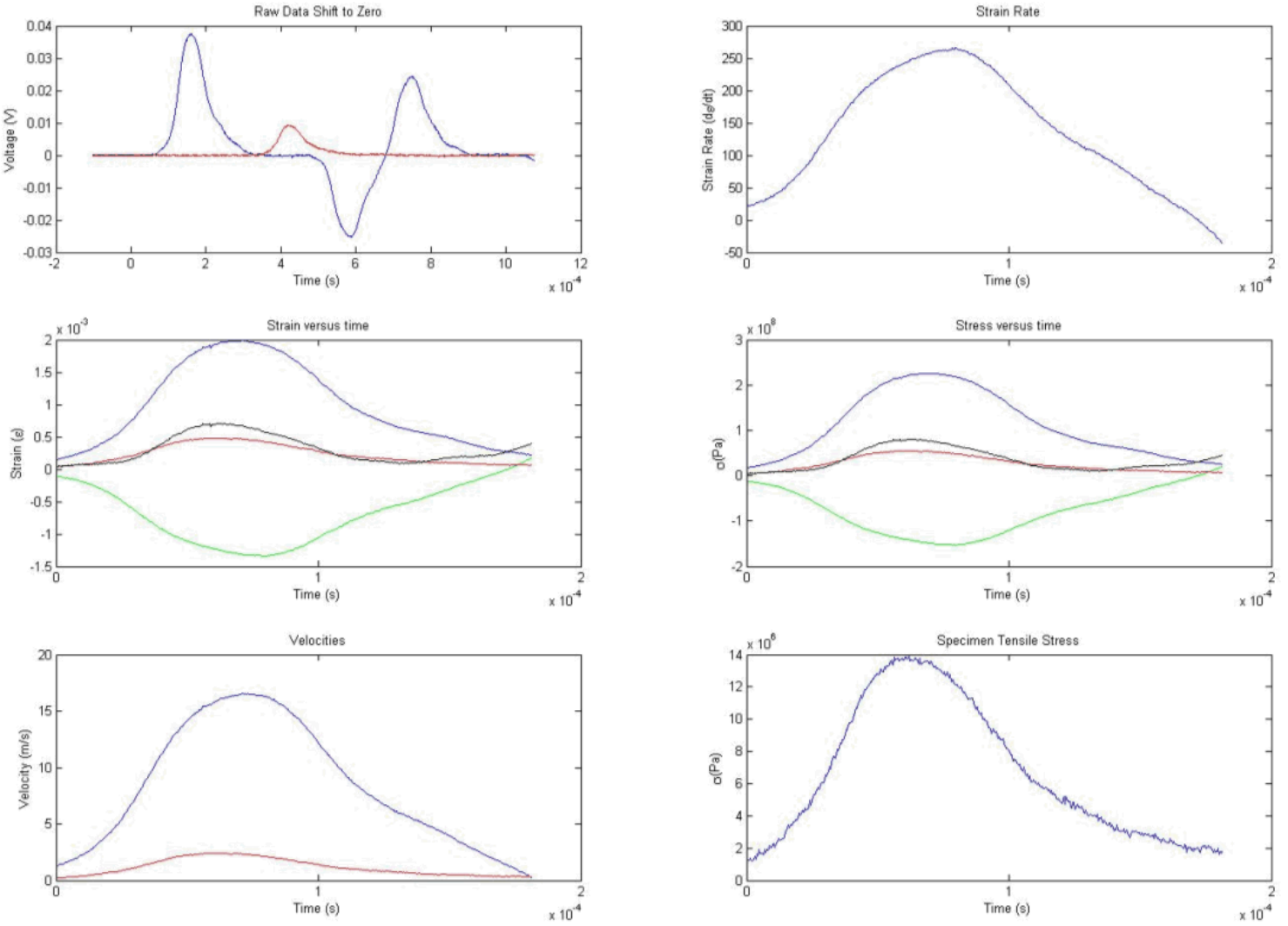

Figure 12. Strain data converted to incident, transmission bar, and specimen strain and stress for specimen SPE-BR-01.

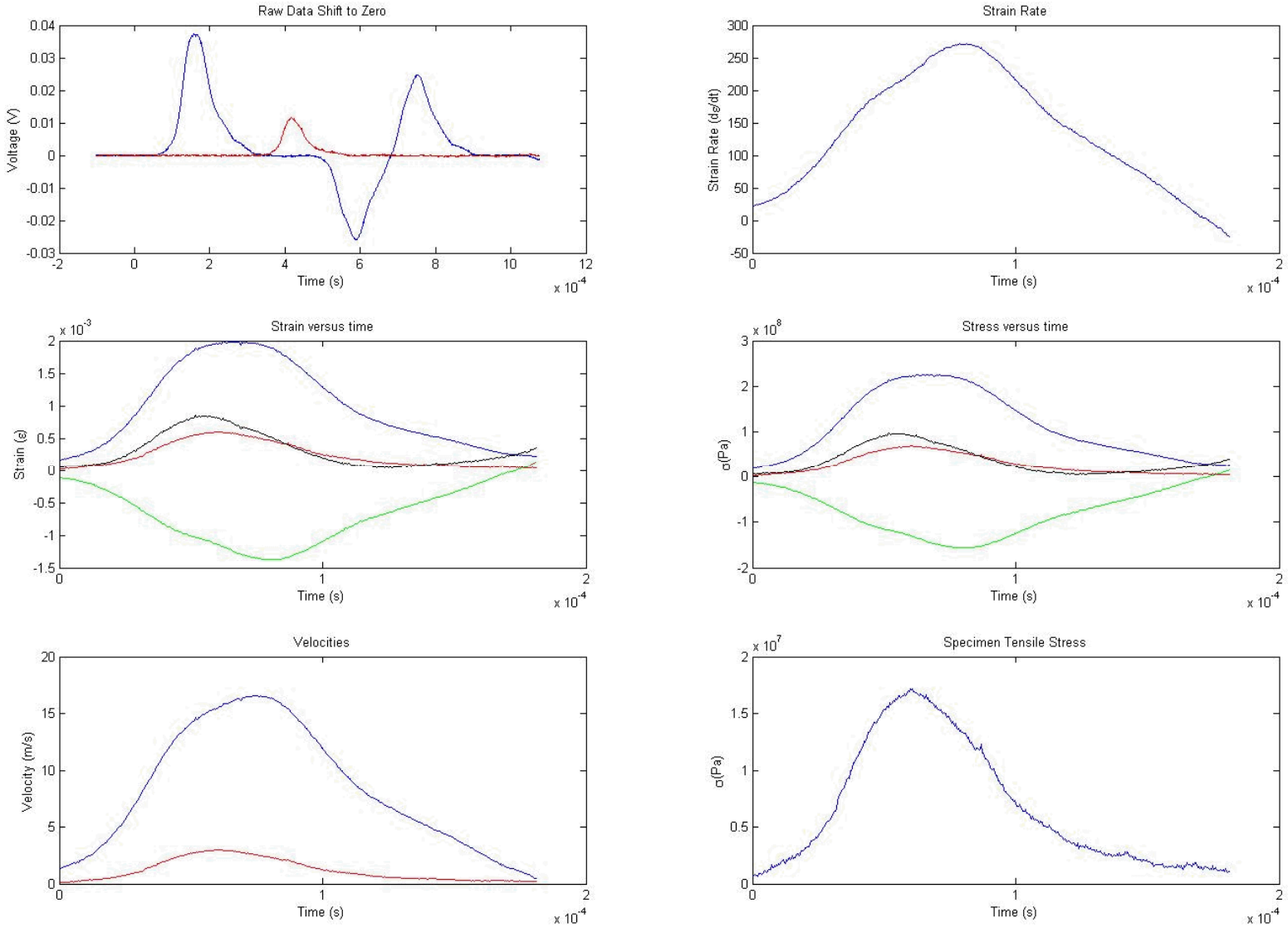

Figure 13. Strain data converted to incident, transmission bar, and specimen strain and stress for specimen SPE-BR-02.

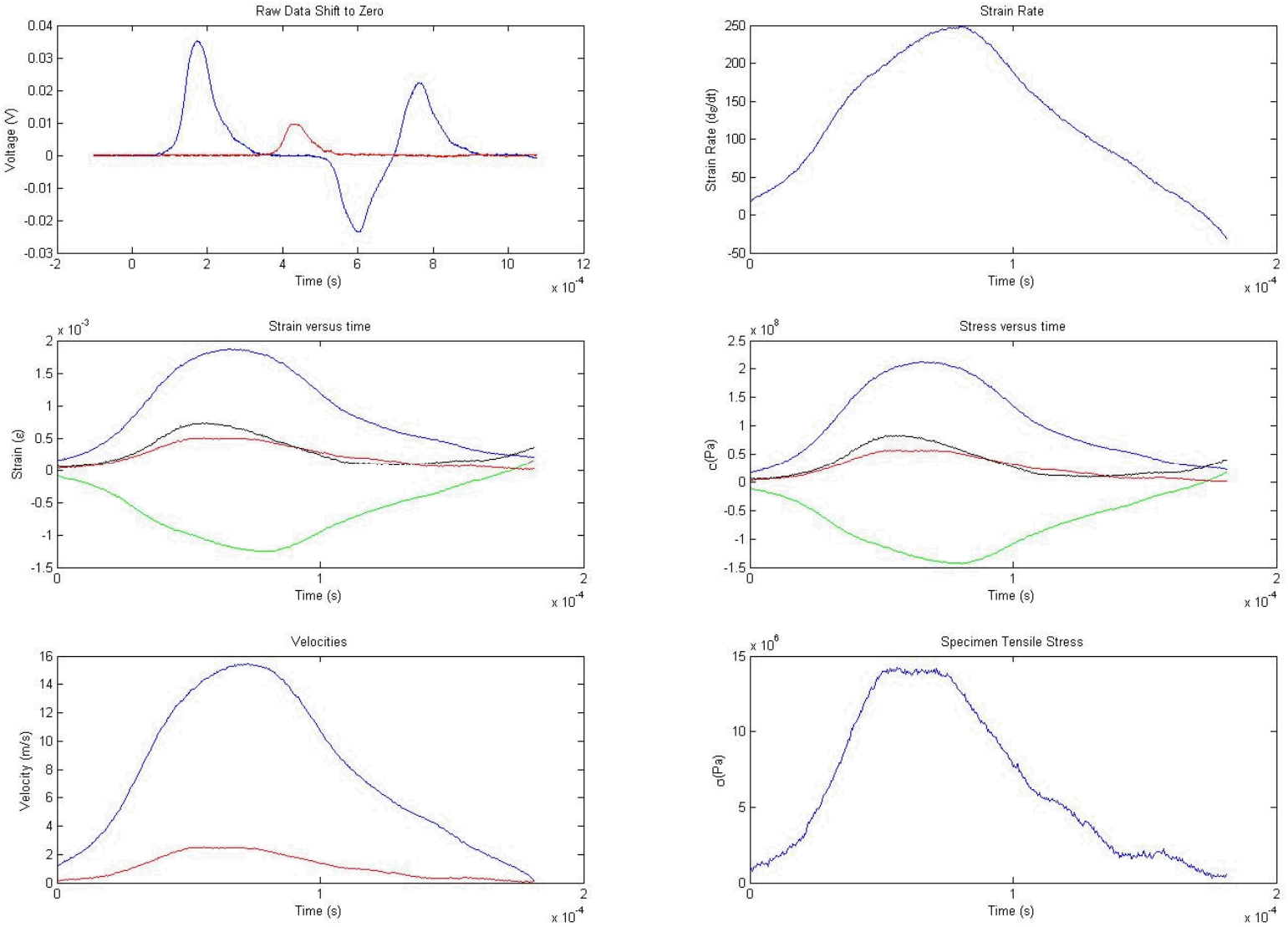

Figure 14. Strain data converted to incident, transmission bar, and specimen strain and stress for specimen SPE-BR-03.

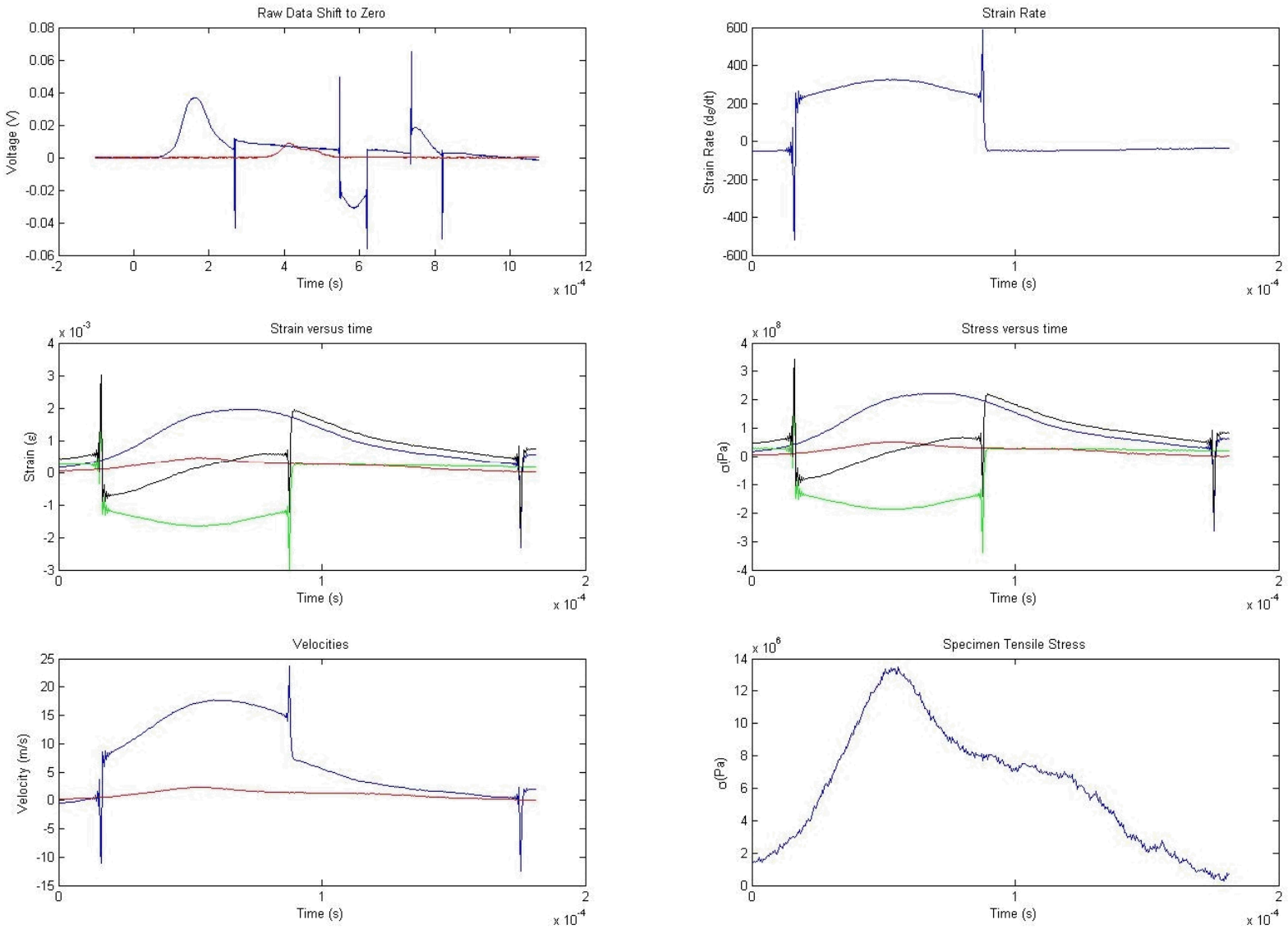

Figure 15. Strain data converted to incident, transmission bar, and specimen strain and stress for specimen SPE-BR-04.

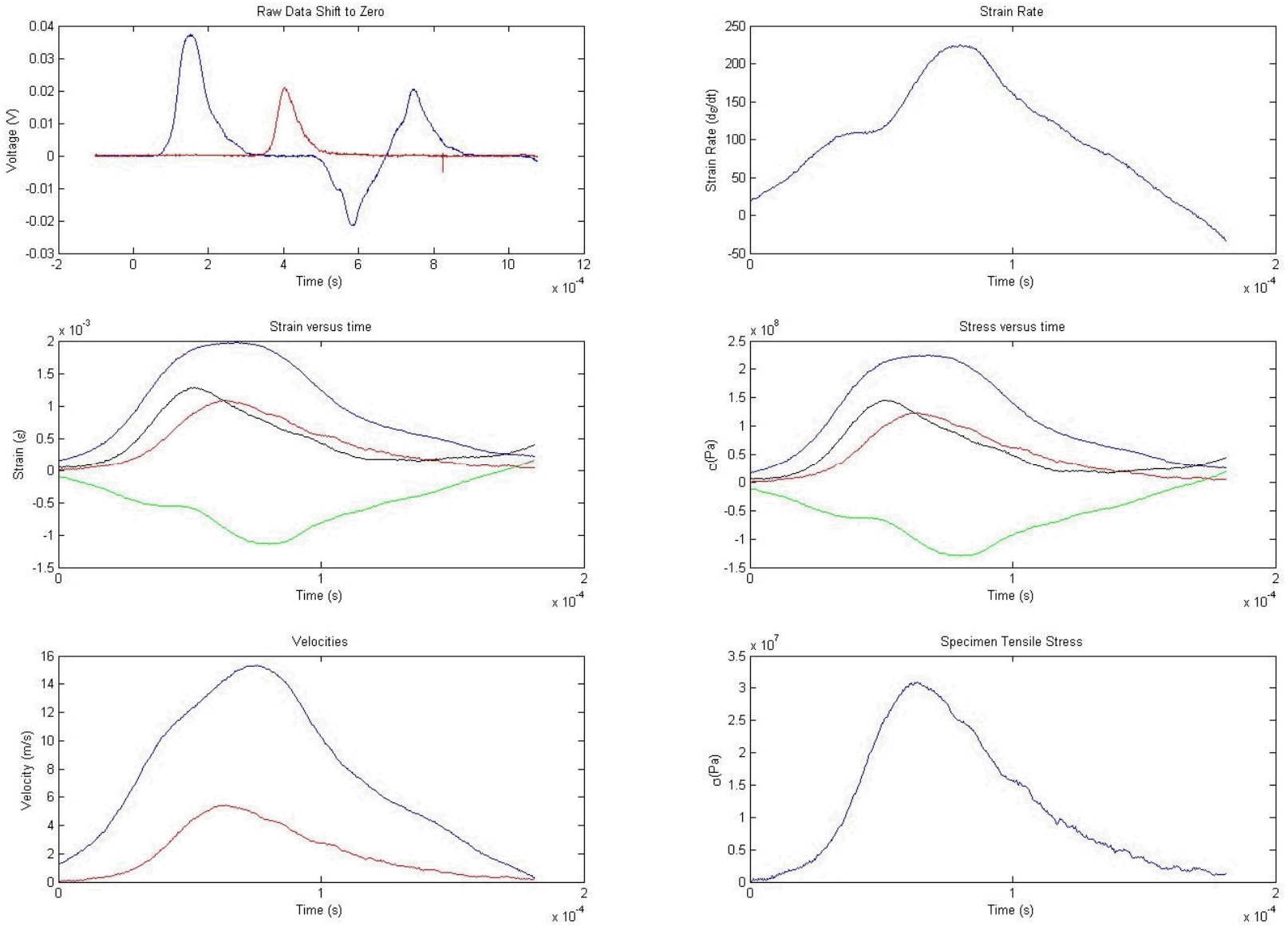

Figure 16. Strain data converted to incident, transmission bar, and specimen strain and stress for specimen SPE-BR-05.

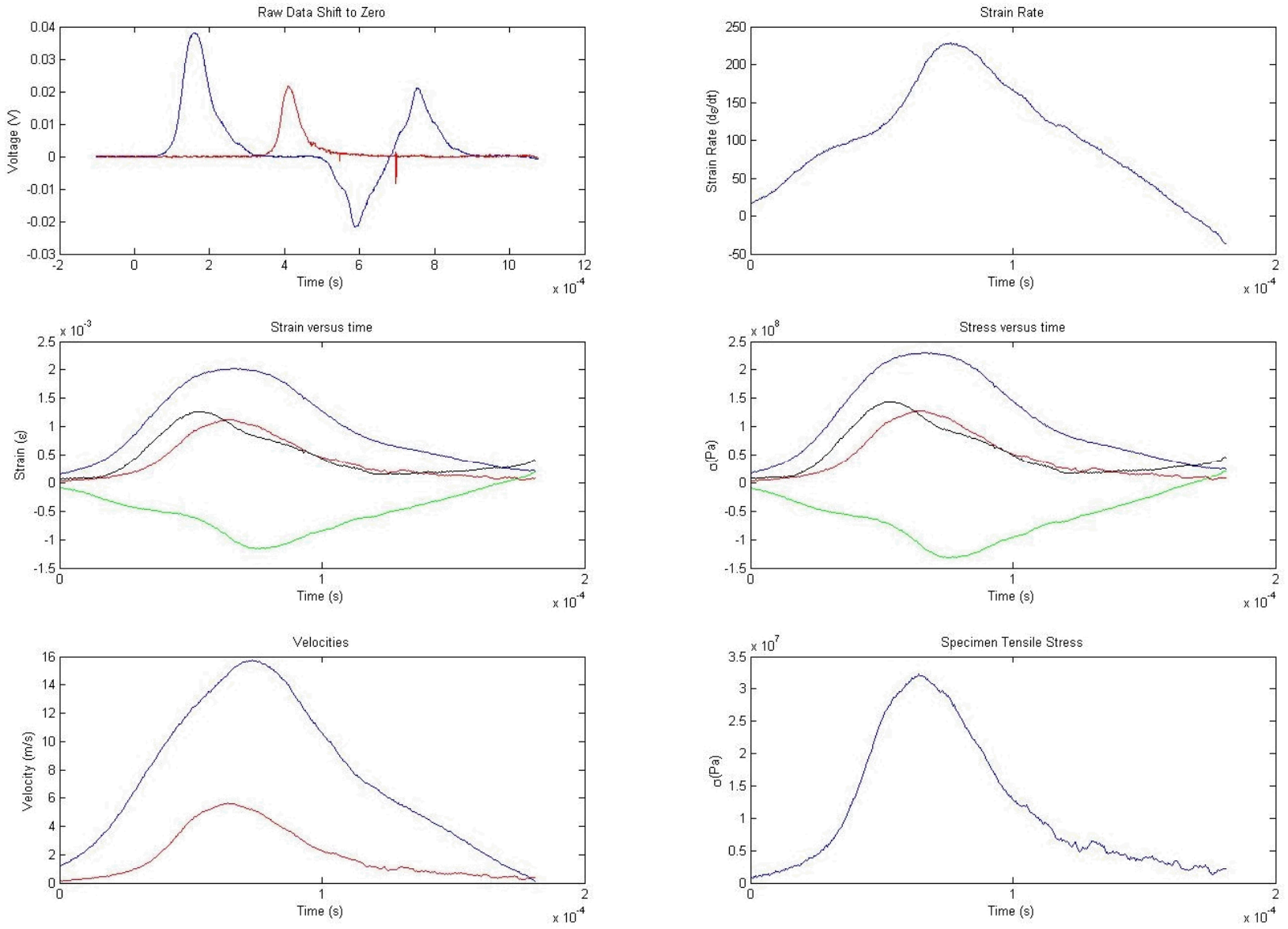

Figure 17. Strain data converted to incident, transmission bar, and specimen strain and stress for specimen SPE-BR-06.

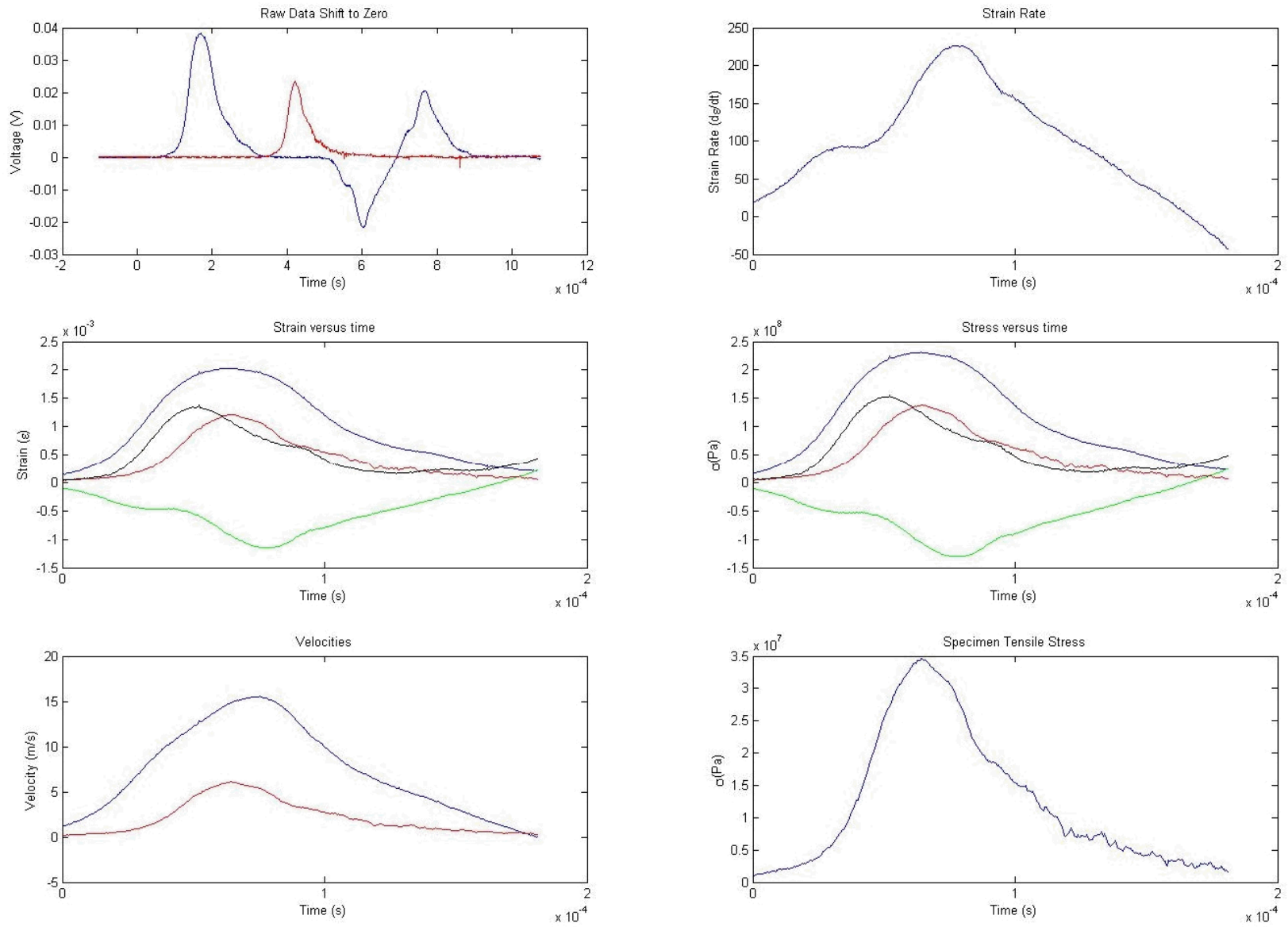

Figure 18. Strain data converted to incident, transmission bar, and specimen strain and stress for specimen SPE-BR-07.

Sandia National Laboratories is a multi-program laboratory managed and operated by Sandia Corporation, a wholly owned subsidiary of Lockheed Martin Corporation, for the U.S. Department of Energy's National Nuclear Security Administration under contract DE-AC04-94AL85000.

The Source Physics Experiments (SPE) would not have been possible without the support of many people from several organizations. The authors wish to express their gratitude to the SPE working group, a multi-institutional and interdisciplinary group of scientists and engineers from National Security Technologies (NSTec), Lawrence Livermore National Laboratory (LLNL), Los Alamos National Laboratory (LANL), Sandia National Laboratories (SNL), the Defense Threat Reduction Agency (DTRA), and the Air Force Technical Applications Center (AFTAC). Deepest appreciation to Msrs. Bob White and Ryan Emmitt (NSTec) for their tireless support on the seismic array and to the University of Nevada, Reno (UNR) for their support with the seismic network and data aggregation. Thanks to U.S. Geological Survey (USGS), the Incorporated Research Institutions for Seismology (IRIS) Program for Array Seismic Studies of the Continental Lithosphere (PASSCAL) Instrument Center, Lawrence Berkeley National Laboratory (LBNL), and Dr. Roger Waxler (University of Mississippi) for instrumentation partnership. The author(s) also wish to thank the National Nuclear Security Administration, Defense Nuclear Nonproliferation Research and Development (DNN R&D) for their sponsorship of the National Center for Nuclear Security (NCNS) and its Source Physics Experiment (SPE) working group. This work was sponsored by the NNSA under award number DE-AC52-06NA25946.

Copy to:

S. Bauer	6914
R. Abbott	6913
T. McDonald	5736